Electronic transport in carbon nanotubes: Diffusive and localized regimes

P. A. Sundqvist, F. J. Garcia-Vidal,* and F. Flores
Departamento de Física Teórica de la Materia Condensada, Universidad Autónoma de Madrid, E-28049 Madrid, Spain
(Received 22 July 2008; revised manuscript received 7 September 2008; published 20 November 2008)

A fully self-consistent analysis of Boltzmann's equations for electrons and phonons is used to study how the resistance of single-walled carbon nanotubes evolves as a function of its length. We demonstrate that the population of hot optical phonons controls the electronic transport of short nanotubes, whereas acoustical phonons take the leading role when the nanotube is very long. In this limit of long tubes, we also analyze the interplay between the diffusive and localized transport regimes when the electron mean-free path and the localization length due to impurities are comparable.

DOI: 10.1103/PhysRevB.78.205427 PACS number(s): 73.63.Fg, 73.23.−b

Carbon nanotubes are ideal one-dimensional systems where both basic science and nanodevice applications naturally merge.[1–7] Their electronic properties are strongly dependent on small structural variations, defects, and also on intrinsic properties as the electron-phonon interaction. In particular, their metallic or insulating character is determined by the chirality of the carbon atoms forming the nanotube. In this paper we analyze the transport properties of metallic single-walled carbon nanotubes (SWNT).

The electronic transport properties of these nanotubes roughly present three distinct regimes: (a) ballistic,[8] (b) diffusive,[9–12] and (c) localized.[13,14] Three different lengths define the appearance of these regimes: L is the nanotube length, L_0 is the localization length, and λ is the electron mean-free path. In SWNTs this mean-free path is mainly controlled by the electron-phonon interaction. If $L \ll L_0, \lambda$, electrons propagate ballistically between the two electrodes, and because of the two channels involved, the electrical resistance, R, can be simply written as $2R=R_0$, with R_0 being the quantum of resistance. If $\lambda \ll L, L_0$, the transport process is controlled by the diffusive propagation of electrons and the resistance exhibits a linear dependence with L, $2R=R_0(1+L/\lambda)$. Finally, the strong Anderson localization regime in SWNTs emerges when $L_0 \ll L < \lambda$ and is characterized by an exponential law for R, $2R=R_0 \exp(L/L_0)$.

In this paper we will discuss theoretically the transport properties of SWNTs in both the diffusive and localized regimes. Regarding the diffusive regime, we present a fully self-consistent analysis of the propagation of electrons along a (10, 10) SWNT taking into account their interaction with both acoustical and optical phonons. In particular, we discuss in detail how the population of hot optical phonons modifies the electron mean-free path[15] and demonstrate that optical phonons get decoupled from electrons for long enough SWNTs. In this limit, electron scattering with acoustical phonons determines the SWNT resistance. An interesting case appears above this limit (very long tubes, $L > 50$ μm) where even a very low density of defects can modify the transport properties of SWNTs. We will show how, if the three characteristic lengths are such that $L_0 < \lambda < L$, the electronic transport in SWNTs enters into an intermediate regime in which the resistance depends on the length as $2R=R_0(1+L/\lambda)\exp(\lambda/L_0)$, in good agreement with very recent experimental evidence.[16]

In the diffusive regime, the nanotube resistance depends critically on the applied bias, V, since optical phonons of energy ϵ_{opt} ($\epsilon_{\text{opt}}=0.18$ eV) can only be excited if $eV > \epsilon_{\text{opt}}$. For $eV < \epsilon_{\text{opt}}$, only acoustical phonons are operative and then $2R=R_0(1+L/\lambda_{\text{ac}})$, λ_{ac} being the electron mean-free path associated with acoustical phonons. In the opposite case ($eV > \epsilon_{\text{opt}}$), both types of phonons play a competing role in the diffusive regime. Notice that at room temperature, λ_{ac} is around 1 μm whereas its optical counterpart, λ_{opt}, is of the order of 50 nm. Therefore, for small L and high biases, R presents a linear dependence with L and the slope is determined by λ_{opt}. For large enough L, however, the applied bias varies very smoothly along the nanotube and optical phonons are excited less effectively. This competing effect between acoustical and optical phonons was analyzed in Ref. 17 by solving self-consistently Boltzmann's equation for electrons along the nanotube. In this analysis, optical phonons were not treated at the same level of consistency and the bias-dependent $\lambda_{\text{opt}}(V)$ was fitted to experimental data. This deficiency is important because the population of hot optical phonons determines the scattering length of the electron-phonon interaction.[15]

In our study of the diffusive regime, we have solved self-consistently the two semiclassical Boltzmann's equations[18] either for electrons (two channels) or for optical phonons (which are assumed to have a constant energy, ϵ_{opt}). Acoustical phonons contribute to the electron-phonon scattering but they are assumed to be in thermal equilibrium with the environment. In our semiclassical model for electrons, for a given voltage, the energy window between $E_{\text{max}}=\epsilon_{\text{opt}}$ and $E_{\text{min}}=-eV-\epsilon_{\text{opt}}$, is discretized into N levels (around 80 to achieve convergence). We analyze, using Boltzmann's equation for each energy, E, the local distribution functions, $n^+(x,E)$ and $n^-(x,E)$, representing electrons traveling at constant Fermi velocity, v_F, along the x positive and negative directions of the one-dimensional nanotube (x measures the distance along the SWNT). The corresponding hole distributions are $p^{\pm}(x,E)=1-n^{\pm}(x,E)$. Along their path, electrons will be scattered by optical and acoustical phonons (see Fig. 1). We quantify the interaction with the optical phonons by means of the functions $H^{\pm}_{\text{opt}}$ and $G^{\pm}_{\text{opt}}$, where $H^{\pm}_{\text{opt}}(x,E)$ describes the probability for an electron of energy E (within a length segment dx located at x) of jumping into another energy level after the absorption or emission of an optical phonon. To account for processes in which electrons of different

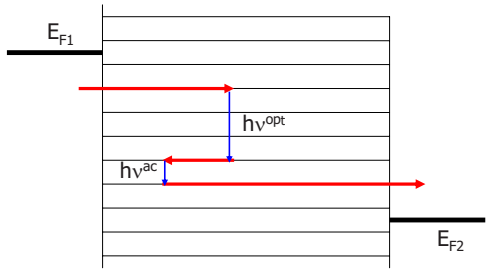

FIG. 1. (Color online) Schematic picture showing the discretized electron levels in the nanotube. In our model, electrons can emit (or absorb) optical phonons of energy $h\nu^{\mathrm{opt}}$, and emit acoustical phonons of energy $h\nu^{\mathrm{ac}}$. All these processes yield, in a self-consistent solution, the electron distribution function, $n(x,E)$ and the optical phonon distribution function, $n_B^{\mathrm{opt}}(x)$. For a nanotube, all electrons move with a constant velocity, v_F, even if their energy w.r.t. the local chemical potential, $E-\mu(x)$, changes.

energies jump into the level of energy E, we use the function $G_{\mathrm{opt}}^{\pm}$. In a similar way, electrons can also be scattered by acoustical phonons, this process characterized by $H_{\mathrm{ac}}^{\pm}$ and $G_{\mathrm{ac}}^{\pm}$. Boltzmann's equations for the electron distributions, $n^{+}(x,E)$ and $n^{-}(x,E)$, are

$$\pm\frac{dn^{\pm}}{dx} = -n^{\pm}(H_{\mathrm{opt}}^{\pm}+H_{\mathrm{ac}}^{\pm}) + p^{\pm}(G_{\mathrm{opt}}^{\pm}+G_{\mathrm{ac}}^{\pm}), \tag{1}$$

where we have omitted the x and E dependence for the sake of brevity. Equation (1) describes how n^{+} and n^{-} evolve as a function of x, for constant energy, E, and constant velocity, v_F (see Fig. 1); as the energy is constant along the trajectory, no contribution from $\frac{\partial n^{\pm}}{\partial E}$ appears in that equation. Moreover, we assume local charge neutrality conditions; this determines the local chemical potential, $\mu(x)$, and the electron momentum by the equation $E-\mu(x)=\pm kv_F$. The mathematical expressions for $H_{\mathrm{opt}}^{\pm}$ and $G_{\mathrm{opt}}^{\pm}$ are

$$H_{\mathrm{opt}}^{\pm}(E) = \frac{1}{\lambda_{\mathrm{opt}}}\{(1+n_B^{\mathrm{opt}})[\bar{\alpha}p^{\mp}(E^{-})+\alpha p^{\pm}(E^{-})] + n_B^{\mathrm{opt}}[\bar{\alpha}p^{\mp}(E^{+})+\alpha p^{\pm}(E^{+})]\}, \tag{2}$$

$$G_{\mathrm{opt}}^{\pm}(E) = H_{\mathrm{opt}}^{\pm}(E;p^{\pm}\to n^{\mp},E^{\pm}\to E^{\mp}), \tag{3}$$

where $\alpha(\bar{\alpha}=1-\alpha)$ describes the forward (backward) scattering rate associated with the interaction between electrons and optical phonons. According to theoretical calculations in Ref. 18, α is close to 0.25. In Eqs. (2) and (3), the population of optical phonons is characterized by the function $n_B^{\mathrm{opt}}(x)$. In Eq. (2), the first term with the factor $(1+n_B^{\mathrm{opt}})$ accounts for the emission of an optical phonon (final energy, $E^{-}=E-\epsilon_{\mathrm{opt}}$), while the second one with the factor n_B^{opt} describes the absorption of an optical phonon (final energy, $E^{+}=E+\epsilon_{\mathrm{opt}}$). The different terms appearing in Eq. (3) have similar interpretations. In Eq. (2), λ_{opt} includes all the optical phonons, longitudinal and transversal,[18] contributing to the electron-phonon scattering rate. From Ref. 18, for a (10, 10) carbon nanotube, $\lambda_{\mathrm{opt}}\approx 85$ nm. In our case, the best fitting to the experimental data is obtained, however, with $\lambda_{\mathrm{opt}}\approx 50$ nm (see below).

As expressed in Eq. (1), longitudinal acoustical phonons

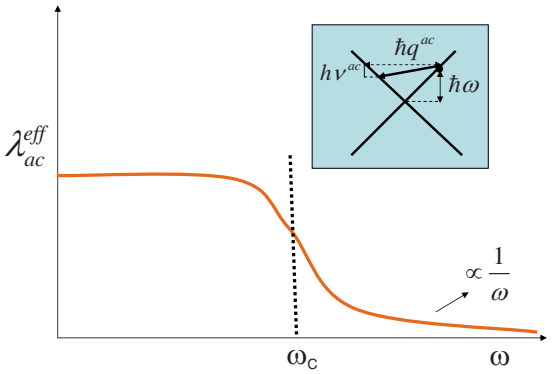

FIG. 2. (Color online) Qualitative behavior of $\lambda_{\mathrm{ac}}^{\mathrm{eff}}$ as a function of the electron energy, $\hbar\omega=E-\mu(x)$. The inset shows one electron of energy $\hbar\omega$ being backscattered by acoustical phonons of energy $h\nu^{\mathrm{ac}}$ and momentum $\hbar q^{\mathrm{ac}}$.

also contribute to the electron-phonon scattering rate, although, being this process a quasielastic one, in our calculations we only consider backscattering. Accordingly, we take $\alpha=0$ in the corresponding equations for $H_{\mathrm{ac}}^{\pm}$ and $G_{\mathrm{ac}}^{\pm}$, analogous to Eqs. (2) and (3),

$$H_{\mathrm{ac}}^{\pm}(E) = \frac{1}{\lambda_{\mathrm{ac}}}[(1+n_B^{\mathrm{ac}})p^{\mp}(E^{-}) + n_B^{\mathrm{ac}}p^{\mp}(E^{+})] \tag{4}$$

$$G_{\mathrm{ac}}^{\pm}(E) = H_{\mathrm{ac}}^{\pm}(E;p^{\pm}\to n^{\mp},E^{\pm}\to E^{\mp}), \tag{5}$$

The inset of Fig. 2 shows how electrons above $\mu(x)$ are backscattered by acoustical phonons; momentum and energy conservation yields the phonon energy, $h\nu^{\mathrm{ac}}$, as a function of the electron energy measured with respect to the local Fermi energy, $\hbar\omega$ $[\hbar\omega=E-\mu(x)]$: $h\nu^{\mathrm{ac}}=2\hbar v_s\omega/v_F$, with v_s and v_F being the acoustical phonon and electron velocities, respectively. It is known that $1/\lambda_{\mathrm{ac}}$ is proportional to q^2/ν^{ac},[19] with q being the phonon momentum and $\nu^{\mathrm{ac}}=qv_s$. For the quasielastic acoustical phonons, $p^{\mp}(E^{-})\approx p^{\mp}(E^{+})$, and Eqs. (4) and (5) can be well approximated by

$$H_{\mathrm{ac}}^{\pm}(E) = \frac{1}{\lambda_{\mathrm{ac}}}(1+2n_B^{\mathrm{ac}})p^{\mp}(E^{-}), \tag{6}$$

$$G_{\mathrm{ac}}^{\pm}(E) = \frac{1}{\lambda_{\mathrm{ac}}}(1+2n_B^{\mathrm{ac}})n^{\pm}(E^{+}), \tag{7}$$

in such a way that an effective λ_{ac} can be introduced as

$$\frac{1}{\lambda_{\mathrm{ac}}^{\mathrm{eff}}} = \frac{1}{\lambda_{\mathrm{ac}}}(1+2n_B^{\mathrm{ac}}) \tag{8}$$

where

$$n_B^{\mathrm{ac}} = \frac{1}{\exp\left(\frac{h\nu^{\mathrm{ac}}}{k_BT}\right)-1}. \tag{9}$$

Now we have to distinguish between two limits depending on the ratio between k_BT and $h\nu^{\mathrm{ac}}$. In the low-T limit $(h\nu^{\mathrm{ac}}\gg k_BT)$, as $n_B^{\mathrm{ac}}\to 0$, $1/\lambda_{\mathrm{ac}}^{\mathrm{eff}}\approx 1/\lambda_{\mathrm{ac}}$ is proportional to $h\nu^{\mathrm{ac}}$, i.e., to $\hbar\omega$. In the opposite limit $(h\nu^{\mathrm{ac}}\ll k_BT)$, n_B^{ac}

$\approx k_B T/h\nu^{ac}$, and $1/\lambda_{ac}^{eff}=2k_B T/(h\nu^{ac}\lambda_{ac})$, independent of $h\nu^{ac}$ and proportional to $k_B T$. Figure 2 shows schematically λ_{ac}^{eff} as a function of $\hbar\omega$, the energy of the incoming electron. For $\hbar\omega_C=\frac{v_F}{2v_s}h\nu^{ac}=\frac{v_F}{2v_s}k_B T$, λ_{ac}^{eff} has a crossover from a constant value (proportional to $k_B T$) to a $1/\omega$ dependence. At room temperature, $\hbar\omega_C$ is of the order of 0.75 eV, and in our calculations at that temperature we can then take λ_{ac}^{eff} as a constant value that will be fitted to the behavior of the resistance at very low voltage. In the second part of this paper, we are going to consider a low-T case, and this approximation will be reconsidered. In addition, as the relevant acoustical phonon energies are between 0 and $k_B T$, we take, for the sake of simplicity, an energy close to 25 meV as the mean energy of the excited acoustical phonons.

Boltzmann's equation for the optical phonon distribution, $n_B^{opt}(x)$, can be written as

$$\frac{\partial n_B^{opt}}{\partial t}+v_{opt}\frac{\partial n_B^{opt}}{\partial x}=\frac{1}{\tau_{opt}}[(1+n_B^{opt})S_{\downarrow}-n_B^{opt}S_{\uparrow}]-\frac{n_B^{opt}}{\tau_{th}}, \tag{10}$$

where τ_{th} represents the thermalization time for optical phonons, which contains contributions from nonlinear decaying processes to acoustical phonons and from heat exchange with the substrate. On the other hand, τ_{opt} is the lifetime of the optical phonons in their interaction with electrons, $\lambda_{opt}=v_F\tau_{opt}$. The magnitudes $S_{\downarrow}$ and $S_{\uparrow}$ account for the generation and absorption rates of the optical phonons, respectively. These quantities depend on the electronic distribution functions, n^+ and n^-, as follows:

$$S_{\downarrow}(x)=\sum_E\{\bar{\alpha}[n^+(E)p^-(E^-)+n^-(E)p^+(E^-)]+\alpha[n^+(E)p^+(E^-)+n^-(E)p^-(E^-)]\}, \tag{11}$$

where the sum extends over all the energy levels. $S_{\uparrow}(x)$ can be obtained by just replacing E^- by E^+. In our approach we assume to have optical phonons of constant energy which implies zero group velocity ($v_{opt}=0$). Then, under stationary conditions ($\partial t\to 0$), Eq. (10) simplifies to

$$n_B^{opt}(x)=\frac{\xi S_{\downarrow}}{1+\xi[S_{\uparrow}(x)-S_{\downarrow}(x)]}, \tag{12}$$

where $\xi=\tau_{th}/\tau_{opt}$. In our calculations we will use ξ as a fitting parameter to available experimental data. Then, our electronic transport problem (for a fixed nanotube length and applied bias) is just to solve self-consistently Eq. (1) for $n^{\pm}(x,E)$ and Eq. (12) for $n_B^{opt}(x)$. In our calculations, we take room temperature (300 K) and assume λ_{opt}, λ_{ac}^{eff}, and ξ to be known. Once the self-consistent solution is reached, the electronic current-voltage relation, $I(V)$, is obtained from the equation $I(V)=4e/h\int dE[n^+(L,E)-n^-(L,E)]$.

Figure 3 renders the evolution of both the (a) resistance and (b) differential resistance as a function of the length for a (10, 10) SWNT for four voltages (V=0.4, 0.7, 1.0, and 1.5 V). Dots correspond to the experimental values as reported in Ref. 17, whereas full curves show the numerical results emerging from our self-consistent approach. The values for the fitting parameters that lead to this excellent agreement

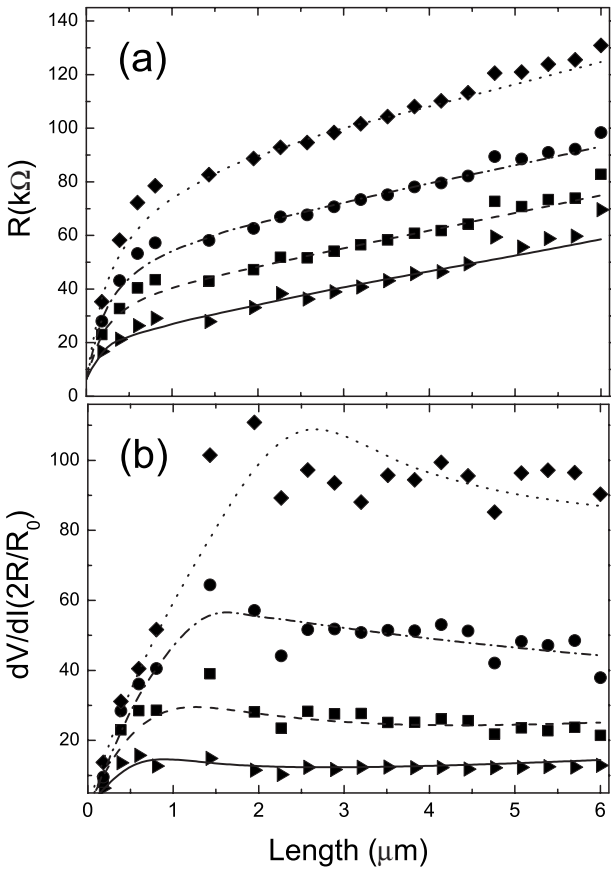

FIG. 3. Resistance (a) and differential resistance, dV/dI, in panel (b) versus L (in microns). Four different values of V are studied: V=0.4 V (full lines), V=0.7 V (dashed lines), V=1.0 V (dash-dotted lines) and V=1.5 V (dotted lines). Dots corresponds to experimental data as reported in Ref. 17.

between theory and experiment are λ_{opt}=50 nm, λ_{ac}^{eff}=650 nm, and ξ=28. Notice that this value for λ_{opt} is a bit smaller than the one obtained from *ab initio* calculations.[18]

The dependence of the population of the hot optical phonons with the applied voltage and length of the nanotube is analyzed in Fig. 4(c). This panel shows how the mean value of $n_B(x)$ increases with voltage, explaining why in Ref. 17, a decaying function of λ_{opt} versus V was needed in order to fit the experimental data. The origin of this behavior is that more optical phonons are excited when the voltage is high, resulting in a shorter effective mean-free path. It is also worth noticing that, for a fixed voltage, $\langle n_B(x)\rangle$ decreases as L is increased. This is due to the fact that when the length of the nanotube is increased, due to the small voltage gradient along the SWNT, electrons have less and less energy to excite optical phonons. This results in a change in behavior for the resistance; for short SWNTs, electron-phonon scattering is dominated by optical phonons, whereas for long tubes, acoustical phonons play the dominant role. This change in behavior is nicely visualized when looking at the evolution of $n^+(x,E)$ at V=1.0 V for two different lengths of the nanotube L=0.5 μm in Fig. 4(a) and L=4 μm in Fig. 4(b). For L=0.5 μm, optical phonons control the distribution function and R while for L=4 μm, acoustical phonons are much more operative. We should mention that the results presented

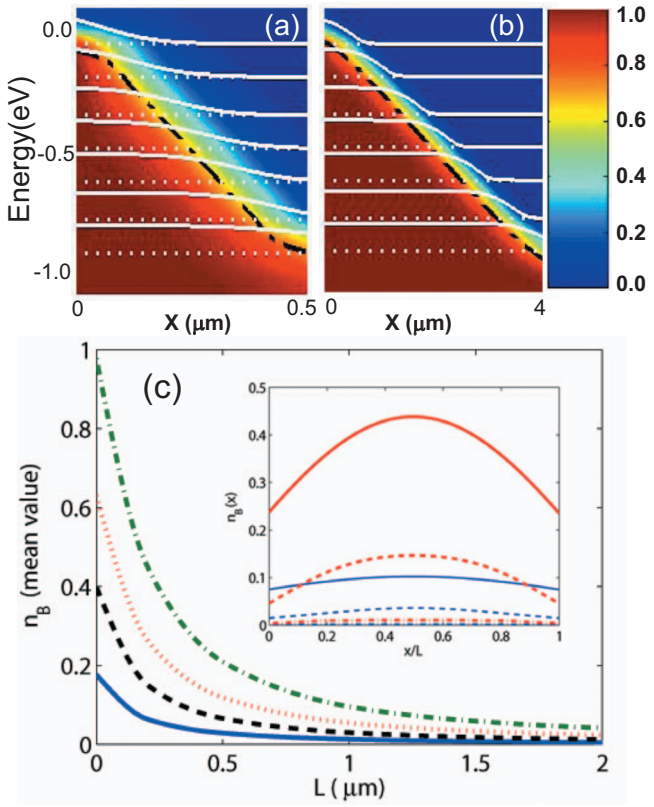

FIG. 4. (Color) Contour plots rendering $n^+(x,E)$ at $V=1.0$ V for two different L's [$L=0.5$ μm in (a) and $L=4$ μm in (b)]. (c) Mean value of $n_B(x)$ for the four voltages analyzed $V=0.4$ V (blue full line), $V=0.7$ V (black dashed line), $V=1.0$ V (red dotted line), and $V=1.5$ V (green dash-dotted line) as a function of the length of the nanotube. Inset shows $n_B(x)$ for two voltages ($V=0.4$ V: blue curves and $V=1.0$ V: red curves) for three different L's ($L=0.1$ μm: full lines; $L=0.5$ μm: dashed lines; and $L=4.0$ μm: dash-dotted lines.

in this paper show some small quantitative differences with those of Ref. 17; this is due to the effects of the hot phonon populations that make λ_{opt} to change with L (in Ref. 17, λ_{opt} was taken constant and different for each bias).

It is convenient to comment also at this point that, apparently, the calculations presented above depend on many different parameters: λ_{ac}^{eff}, λ_{opt}, α, and ξ. However, α is taken from LDA calculations; λ_{ac}^{eff} from the resistance of clean nanotubes at low bias; and λ_{opt} from the resistance at $V=0.4$ V (in this case, there are very few hot phonons and the resistance at small L determines λ_{opt}). Therefore, in our calculations there is only one free parameter (ξ) that we have chosen to give the best fitting to the experimental data. The quality of this fitting shows the good quality of our results. From the previous analysis, we conclude that for long enough SWNTs, the resistance is controlled by acoustical phonons when electrons do not have enough energy to excite optical phonons. λ_{ac}^{eff} is around 1 μm at room temperature, but at very low temperatures ($T=1-5$ K), λ_{ac}^{eff} can be of the order of 100 μm. In this low-temperature limit and for very long tubes, impurities may start to play a role in the electronic transport. In what follows, we will show how this is exactly the case analyzed very recently in the experiments reported in Ref. 16, in which an interplay between the diffusive and localized regimes is taking place.

As mentioned above, three lengths characterize the nanotube resistance behavior: L, λ_{ac}^{eff}, and L_0. Apart from the three canonical regimes already discussed, an unexplored regime emerges when $L_0 < \lambda_{ac}^{eff} < L$. This is a regime in which we can expect to have localized states in the sample; but because of the electron-phonon interaction, we cannot expect a $2R=R_0 \exp(L/L_0)$ law. The crucial point to realize is that if $\lambda_{ac}^{eff} > L$, the localized wave functions extend coherently to the whole system, with peaks in the density of states randomly distributed and having a linewidth proportional to $\exp(-L/L_0)$,[20] which is responsible at the end of the exponential behavior of the resistance. However, when the electron phonon is operative and $\lambda_{ac}^{eff} < L$, the localized states only extend coherently to a region of length λ_{ac}^{eff}. This indicates that the sharp peaks in the density of states in this case would have a linewidth proportional to $\exp(-\lambda_{ac}^{eff}/L_0)$. At the same time, the electron-phonon interaction introduces a diffusive process as electrons move incoherently between localized states. This suggests the introduction of the factor $(1+L/\lambda_{ac}^{eff})$ contributing to the nanotube resistance. All these arguments imply that for $L_0 < \lambda_{ac}^{eff} \ll L$, the nanotube resistance should go as $2R=R_0(1+L/\lambda_{ac}^{eff})\exp(\lambda_{ac}^{eff}/L_0)$. This equation can be easily generalized to include the case $\lambda_{ac}^{eff} \gg L$ by replacing in the exponent $1/\lambda_{ac}^{eff}$ by $1/\lambda_{ac}^{eff}+1/L$. This yields the equation

$$2R = R_0\left(1+\frac{L}{\lambda_{ac}^{eff}}\right)\exp\left[\frac{\lambda_{ac}^{eff}L}{(\lambda_{ac}^{eff}+L)L_0}\right] \tag{13}$$

valid for any values of λ_{ac}^{eff}, L, and L_0, In particular, for $L \to 0$, Eq. (13) yields $2R=R_0[1+L(1/\lambda_{ac}^{eff}+1/L_0)]$, showing that in this limit there is an effective mean-free path, λ_{eff}, given by $1/\lambda_{eff}=1/\lambda_{ac}^{eff}+1/L_0$.

Before comparing the results emerging from Eq. (13) with the experimental data reported in Ref. 16, it is convenient to reconsider our approximation for λ_{ac}^{eff} at low T. As shown in Fig. 2, λ_{ac}^{eff} is proportional to $1/k_BT$ for small $\hbar\omega$; in the other limit, λ_{ac}^{eff} decreases as $1/\omega$. Now if the applied voltage, eV, is much higher than $\hbar\omega_C$, λ_{ac}^{eff} should decrease with that voltage as $1/eV$. This argument indicates that λ_{ac}^{eff} saturates for very short tubes and high bias, and it suggests a length-dependent λ_{ac}^{eff},

$$\lambda_{ac}^{eff}(T) = \frac{\lambda_{ac}^{eff}(T_0)}{T/T_0 + b\lambda_{eff}/L}, \tag{14}$$

where T_0 is the room temperature and b a constant. In Eq. (14), we have introduced the factor λ_{eff}/L that takes into account how the effective bias is reduced for long nanotubes if $\lambda_{eff} < L$; otherwise λ_{eff}/L should be replaced by 1. Note that Eq. (14) is just an interpolation between the two limits of low and high biases. For very low bias, $\lambda_{ac}^{eff}(T) \propto 1/T$, whereas for a high one, λ_{ac}^{eff} takes a constant value. The parameter b in Eq. (14) determines the relative weights of the two limiting values for low and high biases in the final $\lambda_{ac}^{eff}(T)$. Therefore, in principle, this parameter b depends on the applied voltage and will be used in our calculations as a fitting parameter to the experiment.

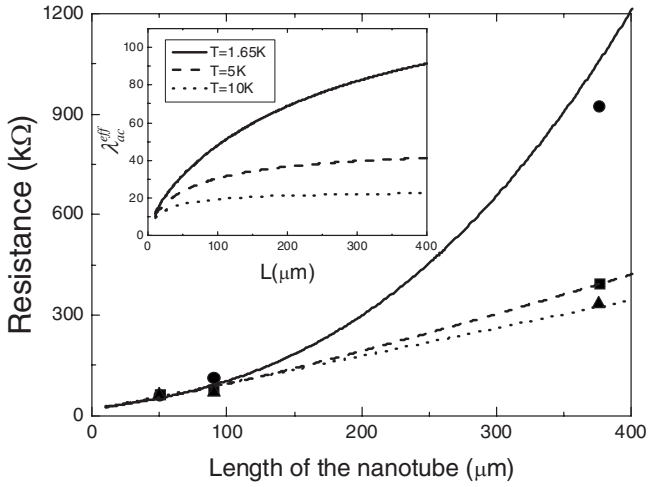

FIG. 5. Theoretical results for R as obtained from Eq. (13) for three different T's: $T=1.65$ K (full line), $T=5$ K (dashed line), and $T=10$ K (dotted line). Dots correspond to the experimental data as reported in Ref. 16. Inset displays the behavior of λ_{ac}^{eff} as a function of L for the three T's analyzed in the main panel.

Figure 5 shows a comparison between Eq. (13) and the experimental data of Ref. 16. We have taken $\lambda_{ac}^{eff}(T_0)=0.8$ μm and $\lambda_{eff}(L\to 0)=7$ μm as in the experiments.[16] As stated above, in our analysis there is only one fitting parameter, $b=0.076$. In this regards, it is worth stressing that the applied bias is 6.4 meV(75 K), this value explaining the importance of the bias correction for λ_{ac}^{eff} as introduced in Eq. (14). The different behaviors for $R(L)$ shown in Fig. 5 for the three temperatures is related to the change in λ_{ac}^{eff} with T (see inset of Fig. 5). In our calculations, we find $L_0=21$ μm and for long tubes ($L=370$ μm), $\lambda_{ac}^{eff}=89$, 41, and 22 μm for $T=1.65$, 5, and 10 K, respectively. It is the high value of λ_{ac}^{eff}/L_0 for $T=1.65$ K found for long tubes, the cause of the rapid increase in the resistance as a function of L for this case. Note that in this limit, $\lambda_{ac}^{eff}\propto 1/T$, and then Eq. (13) leads to $R\propto\exp(1/T)$ when $L\gg\lambda_{ac}^{eff}$. This is exactly the characteristic T dependence for the resistance within the so-called thermally activated electron conduction in the localized regime, as described in Ref. 21. It is also worth mentioning that due to the applied bias, $\lambda_{ac}^{eff}(L\to 0)$ tends to a constant value, independent on T (see inset in Fig. 5). This explains why in the experiments reported in Ref. 16, there is a saturation value for λ_{eff} at very low temperatures.

In conclusion, we have shown how the electron transport in SWNTs depends on the nanotube length and applied bias. For high biases, hot optical phonons control the diffusive regime settled in the nanotube. We have demonstrated that, however, for long enough tubes, acoustical phonons start to dominate the nanotube resistance. A different transport regime appears if L_0, the localization length, is smaller than the electron mean-free path, λ. We have shown that if $\lambda<L$, electron conduction enters to a new transport regime, in which electrons propagate through localized states assisted by phonons. This finding helps completing the landscape of the electronic transport regimes in single-walled carbon nanotubes.

We acknowledge financial support from the Spanish CICYT under Projects No. MAT2005-01298 and No. NAN-2004-09183-C10-07, and the Comunidad de Madrid/Feder Project under Contract No. 07N/0050/2001. We also acknowledge helpful discussions with M. Moreno-Moreno and J. Gómez-Herrero.

*fj.garcia@uam.es

[1] S. Iijima, Nature (London) **354**, 56 (1991).
[2] S. J. Tans, A. R. Verschueren, and C. Dekker, Nature (London) **393**, 49 (1998).
[3] P. M. Ajayan and T. W. Ebbesen, Rep. Prog. Phys. **60**, 1025 (1997).
[4] R. H. Baughman, A. A. Zakhidov, and W. A. de Heer, Science **297**, 787 (2002).
[5] A. Bachtold, P. Hadley, T. Nakanishi, and C. Dekker, Science **294**, 1317 (2001).
[6] A. Javey, J. Guo, Q. Wang, M. Lundstrom, and H. J. Dai, Nature (London) **424**, 654 (2003).
[7] J.-C. Charlier, X. Blase, and S. Roche, Rev. Mod. Phys. **79**, 677 (2007).
[8] C. T. White and T. N. Todorov, Nature (London) **393**, 240 (1998).
[9] Z. Yao, C. L. Kane, and C. Dekker, Phys. Rev. Lett. **84**, 2941 (2000).
[10] J.-Y. Park, S. Rosenblatt, Y. Yaish, V. Sazonova, H. Ustenel, S. Braig, T. A. Arias, P. W. Brouwer, and P. L. McEuen, Nano Lett. **4**, 517 (2004).
[11] A. Javey, J. Guo, M. Paulsson, Q. Wang, D. Mann, M. Lundstrom, and H. Dai, Phys. Rev. Lett. **92**, 106804 (2004).
[12] E. Pop, D. Mann, J. Cao, Q. Wang, K. Goodson, and H. J. Dai, Phys. Rev. Lett. **95**, 155505 (2005).
[13] C. Gomez-Navarro, P. J. de Pablo, J. Gomez-Herrero, B. Biel, F. J. Garcia-Vidal, A. Rubio, and F. Flores, Nature Mater. **4**, 534 (2005).
[14] B. Biel, F. J. Garcia-Vidal, A. Rubio, and F. Flores, Phys. Rev. Lett. **95**, 266801 (2005).
[15] M. Lazzeri, S. Piscanec, F. Mauri, A. C. Ferrari, and J. Robertson, Phys. Rev. Lett. **95**, 236802 (2005).
[16] M. S. Purewal, B. H. Hong, A. Ravi, B. Chandra, J. Hone, and P. Kim, Phys. Rev. Lett. **98**, 186808 (2007).
[17] P. Sundqvist, F. J. Garcia-Vidal, F. Flores, M. Moreno-Moreno, C. Gomez-Navarro, J. S. Bunch, and J. Gomez-Herrero, Nano Lett. **7**, 2568 (2007).
[18] M. Lazzeri and F. Mauri, Phys. Rev. B **73**, 165419 (2006).
[19] J. Ziman, *Electrons and Phonons* (Oxford University Press, New York, 1967).
[20] J. B. Pendry, Adv. Phys. **43**, 461 (1994).
[21] Y. Imry, *Introduction to Mesoscopic Physics* (Oxford University Press, New York, 1998).